A critical study on the experimental determination of stiffness and viscosity of the human triceps surae by free vibration methods

F. París-García[1], A. Barroso[2], J. Cañas[2], J. Ribas[3], F. París[2]

[1] *Faculty of Sport Science, University Pablo de Olavide*

[2] *School of Engineering, University of Seville*

[3] *Faculty of Medicine, University of Seville*

fparis@upo.es, abc@etsi.us.es, pepecanas@etsi.us.es, jribas@us.es, fparis@us.es

Abstract: Muscles and tendons play an important role in human performance. Their mechanical behaviour can be described by analytical/numerical models including springs and dampers. Free vibration techniques are a widely used approach to the in vivo determination of stiffness and viscosity of muscle-tendon complexes (MTC) involved in sport movements. By looking at data reported in literature it appears that visco-elastic properties of the triceps surae MTC are independent of the modality in which free vibration is induced as well as they do not depend on the composition of the population of subjects submitted to the experiments. This research will critically discuss this important aspect focussing in particular on two studies documented in literature. For that purpose, two equipments will be developed to reproduce literature experiments under the assumption that the oscillating part of the body behaves as a single degree of freedom system: the governing degree of freedom is associated to the vertical displacement of the lower leg or to the rotation of the foot around the ankle articulation. Unlike literature, measurements are now conducted on the same population of subjects in order to draw more general conclusions on the real equivalence of results and validity of the mechanical properties determined experimentally. Free vibration tests are accurately simulated by analytical models describing the response of each vibrating system. It is found that if the two measurement protocols are applied to the same population of individuals as it is done in this study, values of visco-elastic properties of MTC extracted from experimental data are significantly different, the differences presenting a convincing consistency. This result is in contrast with literature and confirms the need to evaluate results of free vibration techniques by taking homogeneous bases of comparison.

Keywords: Visco-elastic properties of human triceps surae, in vivo measurements, free vibration techniques, data fitting.

1.- Introduction.

Muscular and tendinous fibres play an important role in improving human performance. Since mechanical behaviour of muscles and tendons resembles a

visco-elastic spring, their response can be described by simple elastic models including spring and damper elements (see, for example, [1]).

Stretch-shortening cycles (SSC) appear in many movements performed by the human body. The muscle-tendon complex (MTC) can work in three different ways [2,3]: (i) excentrically (the muscle opposes elongation); (ii) isometrically (there is neither stretching nor shortening of the muscle); (iii) concentrically (there is a shortening of the muscle). The global mechanical response of MTC depends essentially on two factors: (i) transformation of chemical energy into mechanical energy (i.e. muscular shortening); (ii) efficiency of MTC elastic components in terms of their capacity to store elastic energy at the macroscopic level in the tendons and at the microscopic level in the muscles by means of titin, which is the elastic protein incorporated in the sarcomere that is in turn the smallest functional part of a muscle [4].

In order to establish a direct relationship between the elastic parameters of an MTC (typically stiffness and damping) and its corresponding efficiency in a particular sport discipline, MTC must play an important role in the development of the movements entailed by the discipline in question. For example, the triceps surae (TS), formed by the gastrocnemius (the muscle that generates movement), the soleus (the postural muscle) and the Achilles tendon, is the MTC that permits plantar flexion, a basic phase in the biomechanics of walking [4]. Therefore, TS is of fundamental importance in all sport disciplines involving general displacements.

Experimental determination of MTC viscoelastic characteristics is widely documented in literature. There are two possible approaches to solve this problem: (i) protocols based on the use of cadavers such as, for example, the quick-release method [5], the α-method [6], and the null-point method [7]; (ii) protocols based

on in vivo measurements such as, for example, the quick release method [8,9], application of ultrasounds [10], and free vibration techniques [1,11-14].

The basic idea behind free-vibration techniques that appear to be the approach most commonly used in literature is to induce damped free vibrations in the region of investigation by perturbing through impact another part of the human body. Some characteristic parameter describing the free vibration movement (typically a force) is experimentally measured and then related by a theoretical/analytical/numerical model to visco-elastic properties of tendons and muscles involved in the movement. If free vibration techniques are utilized, it is however necessary to check that experimental measurements are in good agreement with theoretical predictions provided by models within the limits of validity of each assumption made in the modelling stage.

From a careful survey of literature it might appear that visco-elastic properties of the human triceps surae MTC be independent of the modality in which free vibration occurs as well as they do not depend on the composition of the population of subjects submitted to experiments. For example, Fukashiro et al. [12] and Babic and Lenarcic [13] considered different vibration movements: the displacement of the lower leg [12] and the rotation of the foot around the ankle articulation [13], respectively. Although Refs. [12,13] followed the same general principle (i.e. free vibration of the MTC under investigation), the movements monitored in the experimental measurements and, consequently, the associated dynamic equations, are completely different and involve different auxiliary muscular resorts. Furthermore, experiments were carried out on unrelated sets of people. However, visco-elastic properties were found to be quite similar.

In view of this, the present study will critically review the determination of triceps surae visco-elastic parameters documented in [12,13]. The present

investigation is motivated by the fact that although the procedures developed in Refs. [12,13] derive from strong theoretical foundations, the similarity between the results obtained does not seem to have a physical explanation. Therefore, it may be very useful to assess in much deeper detail the real significance of the measured values. The main objective of this paper hence is to assess the true generality and representativity of each procedure in itself as well as to critically compare results. For that purpose, measurements described in [12,13] are reproduced in this research by implementing two experimental set-ups able to carry out the tests. Unlike literature, experimental protocols are carried out on the same population of individuals to avoid further uncertainties in the interpretation of the results.

It is found that visco-elastic properties of the human triceps surae MTC extracted from experimental data now are significantly different. The differences found present a convincing consistency. This result is in contrast with literature data and confirms the need to evaluate results of free vibration techniques by considering homogeneous bases of comparison.

The manuscript is structured as follows. Section 2 describes the free-vibration experimental set-ups, the corresponding theoretical models to simulate dynamic behaviour and the least-square approach used to extract triceps surae visco-elastic properties. Section 3 presents and discusses experimental results in terms of stiffness and viscosity. Finally, Section 4 summarizes the main findings of the study.

2.- Determination of visco-elastic properties of the human triceps surae MTC

In this research, visco-elastic properties of the human triceps surae were determined by conducting in vivo measurements. For that purpose, two experimental setups implementing the free vibration approach were specifically designed and realized. As mentioned previously, the rationale behind free vibration techniques is to originate a free damped vibration of an isolated part of the body. In the present case, the vibration response was controlled by the visco-elastic properties of the TS (Achilles tendon + soleus + gastrocnemius) complex which is assumed to behave as a 1-degree of freedom dynamic system.

The global reaction force developed in the oscillation period was monitored by a load cell and the force values measured over the vibration period were compared with their counterpart predicted by a theoretical model reproducing the 1-degree of freedom dynamic system assumed. In this way, it is possible to build an error function depending on the unknown visco-elastic properties of TS. Finally, stiffness and damping constants can be determined via least-square fitting of experimental data.

The experimental equipments, the corresponding theoretical models, and the least-square fitting procedure are described in detail in the rest of this section.

2.1 TS identification procedure based on the vertical displacement of the lower leg

The experimental apparatus was designed following the measurement approach described in Ref. [12]. The basic idea is to generate a configuration of the human body by allowing in the lower leg a vertical displacement, which will be used as the reference equation of motion. This vertical displacement will be accompanied by rotations of the foot and of the upper leg. The overview schematic of the testing apparatus is shown in Fig. 1. Since the frontal part of the foot is simply supported by a plate, the vertical displacement considered in the measurement involves the rotation of the foot around the articulation of the ankle.

The testing apparatus includes the following main parts (see nomenclature in Fig. 1):

1. Load cell (Interface 1500ASK-300) capturing the evolution of the reaction force as vibration starts. The load cell data acquisition frequency of 1 KHz granted a satisfactory sampling of experimental data. The load capacity of 1500 N is adequate for the typical force values to be measured in the experiments.

2. The impact on the concentrated mass M_w causes the vertical movement of the lower leg as a 1-degree of freedom system. It should be noted that the total oscillating mass M is actually equal to the sum of M_w and the one degree of freedom equivalent mass of the lower limb.

3,4. Elements to accommodate the position of the person currently tested. Both the horizontal and vertical positions can be accommodated in several different locations, which are properly numbered. This allows the chair to be maintained in the same position, for the same person, if the test needs to be repeated. For any morphology of the subject, the three right angles indicated in Fig. 1 must be granted in order to ensure the repeatability of measurements. To this end, the person is asked to maintain the back in contact with the backseat described in the next paragraph.

5. The presence of the vertical backseat ensures, additionally to the former function, that the pressure on the load cell exercised by the foot be constant during measurements. The tested person must keep the back and the shoulders in contact with the backseat in order not to induce pressure variations that might be originated even by very simple movements of the subject's body during the test. Since the type of movement expected in the experiment involves the rotation of the thigh around the hip articulation in the plane of Fig. 1, part of the thigh comes in contact with the seat (of 31 cm depth) as movements develop. However, this did not significantly interfere with the above-mentioned rotation of the thigh because the displacement values observed at the knee level were of the order of mm, involving rotations of the thigh of an order of miliradians (≈0.1 degrees). This small angle, together with the size of the seat (only a very short part of the thigh is in contact with the seat, see Fig.2), make the upper leg to behave freely during the vibration. Furthermore, the thigh-seat contact zone recedes when the leg must hold the equilibrium position just before impact.

6. The simply supported beam allows the loading system to be easily adapted to the anthropometrical features of the subject currently tested.

7. The supporting frame included a triangular structure in order to be enough rigid in the plane of Fig. 1 thus not altering the free vibration behaviour of the system.

Figure 2 shows the testing apparatus and a person ready for the test. It can be seen that the arms of the subject were held in neutral position in order to avoid any interference with the measurement. The setup can be utilized to test indifferently both legs (right and left) without introducing any variation either in the position or in the interpretation of experimental data.

When an impulse is applied to the concentrated mass M_w, the total mass M (i.e. the one-degree of freedom equivalent mass of the lower limb) starts to oscillate vertically as it is indicated in Fig. 1. Figure 3a shows an arbitrary intermediate position for this movement. Whilst distances L (length of the lower leg), R (forefoot distance from the articulation of the ankle) and r (rearfoot distance from the articulation of the ankle) remain constant during the vibration process the length associated to the triceps surae changes.

In this study, the TS complex was schematized according to the classical Hill's model [15] by means of a spring of stiffness k and a damper of constant c. It is important to remark that the parallel elastic component (PEC) present in Hill's model has not been considered in the present study (following [12] and the references therein) as is not likely that the PEC significantly contributes to the induced oscillation movement. Since for the position represented in Fig. 1 (i.e. 90° angle at the knee level) the gastrocnemius muscle does not work, the apparent values of stiffness k and damping c of the TS complex are relative to the soleus muscle and the Achilles tendon. For clarity of representation, the equivalent TS spring-damper system sketched in the figure is inclined by a certain angle with respect to the direction corresponding to the lower leg. However, in the derivation of theoretical model, TS was always considered parallel to the lower leg.

The configurations shown in Fig. 3 are referred to a fixed point corresponding to the contact region between the subject's foot and the load cell measuring the reaction force F.

The mass represented in Fig.3 is the total mass M involved in the movement, which is the sum of the concentrated mass M_w and the one degree of freedom equivalent mass representing in the model the distributed mass of the

lower limb. Thus, M will represent the total one degree of freedom equivalent mass involved in the movement.

The displacements U and u indicated in Fig. 3a are related each other as follows:

$$U = \frac{R}{r}u \qquad (1)$$

The forces involved in the equilibrium around the ankle articulation are indicated in Fig. 3b: the force F_{tf} keeps the tibia-fibula set in compression while the force f keeps the TS complex in tension. From the condition of dynamic equilibrium of the forces schematized in Fig. 3b with respect to the ankle articulation it follows:

$$(I + m_f r_G^2)\frac{d^2\theta}{dt^2} = FR\cos\theta - fr\cos\theta \qquad (2)$$

where: θ is the angle (Fig. 3a) defining the instantaneous position of the foot; I is the momentum of inertia of the foot with respect to its centre of gravity; m_f is the mass of the foot involved in the movement; r_G is the distance between the centre of gravity of the foot and the centre of rotation. Notice that the force corresponding to the weight of the leg and concentrated mass is aligned with the movement, its moment with respect to the axis of rotation being negligible in absolute terms.

The values of parameters in the left hand side (LHS) of Eq. (2) were estimated from [16, 17]. Since these summands of the LHS of Eq. (2) are, in relative terms, much smaller than their counterpart for the right hand side (RHS), Eq. (2) reduces to:

$$FR = fr \qquad (3)$$

The above equation allows the value of the force f passing through the line of action of the TS complex to be obtained once the value of the reaction force F is measured by the load cell and the distances R and r are precisely determined for the tested foot.

The system in Fig. 3a includes two coupled degrees of freedom: the rotation around the ankle articulation and the vertical displacement of the vibrating mass. Since the tibia-fibula set was assumed to be infinitely rigid [18,19], the vertical displacement of the mass M coincided with the vertical displacement of the ankle rotation point. The equivalent dynamic system hence corresponds to the 1-degree of freedom system schematized in Fig. 4a where K and C are the apparent stiffness and the damping coefficient.

By taking as reference the configuration of the system including the external weight, the dynamic equilibrium condition for the total mass M, after the impact, can be expressed as:

$$M\ddot{U} = -KU - C\dot{U} \quad (4)$$

By disaggregating the system (see the scheme of forces in Fig. 4b) it can be written:

$$F = -KU - C\dot{U}(= M\ddot{U}) \quad (5)$$

Should the reference configuration correspond to the instant preceding the application of the weight, a term $-M_s g$ should be added in the RHS of Eq. (4). M_s represents the total static mass of the vibrating system (i.e. the mass that corresponds to the system that is vibrating, before to start the vibration). Notice that this M_s mass does not have to exactly coincide with the total dynamic mass M

involved in the movement. The reason is that whereas the part M_w of M is a concentrated mass, the remaining mass of M is a distributed mass, that of the lower limb. In a system of concentrated parameters, a unique mass, representing infinite points able to have different accelerations, is involved in the equation of motion with a unique value of acceleration. Thus, both masses, static and dynamic, correspond to different concepts. They would coincide if the acceleration was the same in all points of the actual distributed parameters system.

The general solution of the differential equation (4) written for an underdamped system is:

$$U(t) = e^{-\xi\omega t}(A\sin\omega_D t + B\cos\omega_D t) \quad (6)$$

where the constants A and B are determined from the boundary conditions of the problem.

The damping factor ξ is defined as:

$$\xi = \frac{C}{C_c} = \frac{C}{2M\omega} \qquad (7)$$

where C is the damping of the system; C_c is the critical damping of the system; M is the total mass involved in the movement; and ω is the natural frequency of the vibrating system.

The frequency of vibration ω_D of the damped system is:

$$\omega_D = \omega\sqrt{1-\xi^2} \qquad (8)$$

By defining the parameter γ as:

$$\gamma = \xi\omega = \frac{C}{2M} \qquad (9)$$

it is possible to express the vibration frequency ω_D of the damped system as follows:

$$\omega_D^2 = \omega^2 - \gamma^2 \quad (10)$$

The general expression of displacement (6) can be substituted in the equation of dynamic equilibrium (5). It is thus possible to express the total force F acting on the mass M as:

$$F = (M\ddot{U}) = e^{-\gamma t}(A_F \sin \omega_D t + B_F \cos \omega_D t) \quad (11)$$

Where A_F and B_F can be expressed in terms of M, A, B, γ and ω_D as:

$A_F = M\left(2B\gamma\omega_D + A(\gamma^2 - \omega_D^2)\right)$ and $B_F = M\left(-2A\gamma\omega_D + B(\gamma^2 - \omega_D^2)\right)$.

Since the load cell can sense the force (11) plus the action of gravity, the total force F_m measured in the experiments is:

$$F_m = F + M_s g = e^{-\gamma t}(A_F \sin \omega_D t + B_F \cos \omega_D t) + M_s g \quad (12)$$

Because of the presence of weight, the sign of F_m is always negative (i.e. F_m is compressive) while the sign of force F depends on the equilibrium position.

Notice that the variable γ involves (by means of (9)) the dynamic mass M participating in the movement. The static mass M_s could in principle be determined using the load cell, either before the impact or during the steady state period after the attenuation of the signal. Then, the parameters γ, ω_D, A_F, B_F could be determined.

Due to the fact that in the two steady-state periods there always are small oscillations and that both values may be slightly different due to small movements of the subject, the accurate identification of M_s is not a straightforward task. Additionally, due to the dominant role of the concentrated mass in the total dynamic mass, it is expected that the behaviour of the system is correctly represented assuming ($M_s \approx M$), a typical assumption followed in previous papers [12-14].

With this hypothesis, expression (12) includes the unknown parameters γ, ω_D, A_F, B_F and M ($M \approx M_s$) that must be determined with the least-squares fitting procedure described in Section 2.3.

Once these unknown parameters are determined, the values of apparent stiffness K and damping C of the whole system can be determined as follows:

$$K = M(\omega_D^2 + \gamma^2) \qquad (13)$$

$$C = 2\gamma M \qquad (14)$$

Parameters K and C can be related to the apparent stiffness k and damping c of the TS complex. For that purpose, the condition of dynamic equilibrium can be written also for the TS by referring to the load diagram shown in Figure 5 a). An illustration of the TS and its constituents (Soleus, Gastrocnemius and Achilles Tendon), to which Fig. 5a represents, is shown in Figure 5 b).

$$f = -ku - c\dot{u} \qquad (15)$$

By substituting Eqs. (1) and (3) in Eq. (5) and rearranging the expression it follows:

$$f = -\left(\frac{R}{r}\right)^2 Ku - \left(\frac{R}{r}\right)^2 C\dot{u} \qquad (16)$$

Since Eqs. (15) and (16) are equivalent, all terms contained in these expressions must coincide. The following conditions can hence be obtained:

$$k = \left(\frac{R}{r}\right)^2 K \quad , \quad c = \left(\frac{R}{r}\right)^2 C \qquad (17)$$

A very important issue entailed by the above described model is the precise determination of the values of r and R for the tested person. This aspect is discussed in detail in Section 2.3 and Ref. [20].

2.2 TS identification procedure based on the rotation of the foot around the ankle articulation

The experimental apparatus was designed following the measurement approach described in Ref. [13]. The basic idea is to generate a configuration of the human body by allowing only the rotation of the foot around the articulation of the ankle. The overview schematic of the testing apparatus is shown in Fig. 6. The configuration of the equipment may be easily arranged so to have the leg in complete extension thus putting the gastrocnemius in free vibration. However, since the main objective of the present study was to critically compare Refs. [12,13], only the configuration shown in Fig. 6 was considered.

The testing apparatus includes the following main parts (see nomenclature in Fig. 6):

1. The same load cell used in the previous experiments (Interface 1500ASK-300) was utilized to monitor the evolution of the force transferred by the wire during vibration.

2. The impact on the concentrated mass M_w causes the rotation of the foot around the articulation of the ankle as a 1-degree of freedom system. It should be noted that the total oscillating mass M, independently of the foot, is actually equal to the sum of M_w and the mass of the whole system associated to the movement of the wire. As in the previous case, since it may not be an easy task to identify the actual value of M, the total oscillating mass M was included as an additional parameter in the fitting process. The total mass M was located in the same position as M_w (see Fig. 8 later shown in the paper) because its position does not affect the equation of movement. For this load case, the mass m_f of the foot was considered separately. The movement was produced by applying an impulsive load to the mass M_w.

3-4. Elements to accommodate the position of the person currently tested. For any morphology of the subject, the three right angles indicated in Fig. 6 must be granted and the rotation of the foot around the ankle articulation must be the only movement allowed. This ensured the validity of measurements.

5. The system transferring the load from the weight to the foot was comprised of a steel wire and two pulleys. The wire was very stiff with respect to tensile forces and flexible enough with respect to bending in order to easily adapt to the local shape of pulley channel. After several trials, the cross section of the wire was selected as a thin rectangular steel lamina of width 17mm and thickness 0.5 mm. The position of the pulley placed at the level of the foot (i.e. the pulley closest to the foot in the direction of transferred load) was tuneable in height thus allowing the final part of the wire to be held horizontal near the subject's foot.

The disposition presented in Section 2.1 can be used in a natural form for both legs. However, the disposition associated to present procedure, requires either to conceive a unique very complicated device to test both legs, or to design a simpler one, but applicable only to one leg. The second option was selected and a testing apparatus for the right leg, Fig.7, was designed and built. To try to use the apparatus of Fig. 7 to test also left leg would imply the subject to take a forced posture where the right leg would be placed unnaturally in the right side of the structure, what can significantly affect measurements.

In order to derive the theoretical model describing the dynamic behaviour of the system under free vibration the reference scheme of Fig. 8 was considered. The distance R between the origin of the reference system and the line of action of the equivalent force acting on the total mass M, the distance R_G between the origin of the reference system and the centre of gravity of the foot, and the distance r

between the origin of the reference system and action line of the Achilles tendon can be expressed as follows:

$$\begin{aligned} R &= \left| r_F \sin\varphi_F \right| \\ R_G &= \left| r_G \sin\varphi_G \right| \\ r &= \left| r_f \sin\varphi_f \right| \end{aligned} \qquad (18)$$

Under the hypothesis of infinite stiffness of the wire, the condition of momentum equilibrium written with respect to the equilibrium position (i.e. after applying the mass M_w) can be stated as:

$$(I + m_f R_G^2 + MR^2)\ddot{\varphi} = fr \qquad (19)$$

where: I has been previously defined, φ is the angle that defines the position of the foot during the vibration movement and f is the reaction force developed in the MTC.

The reaction force f developed in the MTC is the sum of the contribution of a spring of stiffness k and a damper of damping coefficient c. It can be written:

$$f = -ku - c\dot{u} = -k\varphi r - c\dot{\varphi} r \qquad (20)$$

where the relationship $u=\varphi r$ between φ and u is derived from Fig. 8.

By substituting the last equality of Eq. (20) in the RHS of Eq. (19) and rearranging terms, the dynamic equilibrium equation describing the movement of the system can be obtained:

$$(I + m_f R_G^2 + MR^2)\ddot{\varphi} + cr^2\dot{\varphi} + kr^2\varphi = 0 \qquad (21)$$

Similarly to the previous loading condition, the terms relative to the inertia of the foot are negligible with respect to MR^2. Therefore, Eq. (21) reduces to:

$$MR^2\ddot{\varphi} + cr^2\dot{\varphi} + kr^2\varphi = 0 \qquad (22)$$

The simplifying assumption leading to Eq. (22) makes it unnecessary to measure the position of the centre of gravity of the foot.

The general solution of the differential equation (22) is:

$$\varphi(t) = e^{-\gamma t}(A\sin\omega_D t + B\cos\omega_D t) \qquad (23)$$

hence analogous to the general displacement solution (6) derived in Section 2.1.

The values of γ and ω_D are respectively defined as:

$$\gamma = \frac{cr^2}{2MR^2} \qquad (24a)$$

$$\omega_D^2 = \frac{kr^2}{MR^2} - \gamma^2 \qquad (24b)$$

By combining Eqs. (24), the visco-elastic parameters k and c of the TS complex can be obtained:

$$k = \frac{MR^2}{r^2}(\omega_D^2 + \gamma^2) \quad (25a)$$

$$c = \frac{2MR^2}{r^2}\gamma \quad (25b)$$

In order to determine the values of k and c, one has to determine γ and ω_D first by measuring the force developed in the wire as the impulsive load is applied. This force, which is registered by the load cell, can be expressed as:

$$F_m(t) = M(g + \ddot{\varphi}R) \quad (26)$$

The assumption that $M_s \approx M$ reasoned in Section 2.1 will also be employed in this Section 2.2, as done in (26) with reference to the term $M_s g$.

If the displacement solution of Eq. (23) is derived twice with respect to time the following expression is obtained:

$$\ddot{\varphi}(t) = e^{-\gamma t}(A_a \sin\omega_D t + B_a \cos\omega_D t) \quad (27)$$

Where A_a and B_a can be expressed in terms of A, B, γ and ω_D as:

$A_F = \left(2B\gamma\omega_D + A(\gamma^2 - \omega_D^2)\right)$ and $B_F = \left(-2A\gamma\omega_D + B(\gamma^2 - \omega_D^2)\right)$.

By substituting Eq. (27) in the RHS of Eq. (26), the final expression of the force to be measured is:

$$F_m = F(t) = e^{-\gamma t}(A_F \sin \omega_D t + B_F \cos \omega_D t) + Mg \qquad (28)$$

Where A_F and B_F can be expressed in terms of M, R, A, B, γ and ω_D as:

$A_F = MR\left(2B\gamma\omega_D + A(\gamma^2 - \omega_D^2)\right)$ and $B_F = MR\left(-2A\gamma\omega_D + B(\gamma^2 - \omega_D^2)\right)$.

Expression (28) includes the unknown parameters γ, ω_D, A_F, B_F and M that must be determined with the least-squares fitting procedure described in Section 2.4. Equations (25) must hence be used to evaluate MTC visco-elastic parameters k and c.

Similarly to the loading case previously considered, the values determined for parameters k and c may be strongly sensitive to the ratio R/r. Therefore, once forefoot and rearfoot distances R and r were determined for a subject, special cares must be taken in placing the foot always in the correct position (i.e. the second metatarsal head must be in contact with the transmission device). This position must be the same for both loading cases in order to have a homogenous basis of comparison for the visco-elastic parameters extracted from the two in vivo procedures considered in the study.

2.3. Forefoot and rearfoot distances measurement

A noninvasive procedure based on pedigraphies, to obtain the lever arms of the forefoot (R) and rearfoot (r), has been developed. The procedure has two phases: the first is to obtain a footprint, by means of a pedigraphy, indicating on it a certain number of anatomical references. In a second phase, a procedure for locating the necessary 3 points of reference is followed. The three points,

indicated as *a*, *b* and *c* in Fig. 9 are placed along the longitudinal axis of the foot and their location allows us to obtain the desired lever arms.

Point *a* is located at the position of the resultant of the distribution of pressure in the forefoot. Point *b* represents the intersection point between the projection of the ankle rotation axis and the longitudinal axis of the foot. Finally, *c* represents the projection of the Achilles tendon axis on the footprint plane. In this way, the positions *a*, *b* and *c* determine the distances *R* and *r*, as indicated in Fig. 9. A more detailed description of the procedure can be found in [20].

2.4.- Processing of experimental data and extraction of TS visco-elastic parameters

Reaction force values were recorded by the load cell at regular time intervals. A typical force-time plot is shown in Fig. 10 where the steady-state value finally reached by *F* is denoted as F_{ss}. The plot in Fig. 10 is relative to the measurement protocol described in Section 2.1 and was obtained for a nominal weight of 25 kg. The nominal value of applied load was recovered after the vibration period originated by the impulsive load. The steady-state force value indicated in the figure is about 35 kg, hence 10 kg higher than the nominal weight of 25 kg. This is because of the presence of the weight of the lower leg involved in the vibration process. Notice that all values of the vertical axis are negative due to the fact that the load cell is in compression.

The equivalent force measured by the load cell for the two experimental procedures described in Sections 2.1 and 2.2 always has the same expression (i.e. Eqs. (12) and (28) for, respectively, the first and the second loading case). The instantaneous force value always depends on five parameters: the damping coefficient γ, the vibration frequency of the damped system ω_D, the total mass *M*

involved in the movement (after the identification of M_s and M), and the coefficients A_F and B_F.

In order to determine the unknown parameters listed above, one can minimize the error functional Ω corresponding to the difference between the values of force measured by the cell and their counterpart predicted by numerical models:

$$\Omega = \sum_{i=1}^{n} \left[F_{\exp}(t_{\exp}) - F(\gamma, \omega_D, A_F, B_F, M) \right]^2 \quad (29)$$

where: n is the number of control points (i.e. experimentally recorded data) to be included in the fitting procedure; F_{exp} is the force value experimentally measured at the sampling time t_{exp}; F is the force value predicted by the theoretical model based on the assumption of a 1-degree of freedom system.

The error functional Ω was minimized in the least-square sense. Generally speaking, the fitting procedure should always converge to the global minimum. However, there are some aspects to be considered. In the first place, the probability of reaching the global optimum may depend significantly on the ranges of variation chosen for the five unknown parameters involved in fitting procedure. Furthermore, optimization behaviour may be sensitive to the initial values set for the fitting parameters that should always be chosen in view of their physical meaning or on the basis of previous experience acquired for similar problems. In particular, very accurate estimations of the initial values of M, γ and ω_D can be obtained from the experimental data, the first as the value before (and after) the perturbation, the second as the decay of consecutive peaks of the oscillating signal, and the third, measuring the time interval between consecutive peaks of the signal. Other critical aspects are how to select the time interval in which experimental data must be recorded either in terms of the size and position

of the interval and the number of control points where the error functional Ω must be evaluated.

A sensitivity study was carried out in this research in order to optimize the performance of the fitting procedure. All cases considered in the parametric analysis are summarized by Fig. 11. The experimental curve taken as an example in Fig.11 corresponds to the first procedure (Section 2.1), reason by which the reaction force (data in the vertical axis) presents negative values, the load cell being always in compression. The following general nomenclature was adopted: case.subcase ($t_{initial}$, t_{final}, density). Density=1 means that all data points were used to build the error functional while density=0.1 means that only 1 data point out of every 10 data points was used.

Cases 1) For fixed sizes (i.e. between 1.4 and 1.7 s) of the data time interval, different time origins were chosen for the experimental force-time plots. Subcase "a" corresponds to $t_{initial}$=1.4 s; subcase "b" corresponds to $t_{initial}$=1.5 s; subcase "c" corresponds to $t_{initial}$=1.6 s; subcase "d" corresponds to $t_{initial}$=1.7 s.

Cases 2) For a fixed time origin (i.e. 1.4 s), different sizes of the time interval were considered. Subcase "a" corresponds to a time interval of 0.5 s; subcase "b" corresponds to a time interval of 0.6 s; subcase "c" corresponds to a time interval of 0.7 s; subcase "d" corresponds to a time interval of 0.8 s.

Cases 3) For a fixed origin (i.e. 1.4 s) and size (i.e. 2.2 s) of the time interval, different densities of the experimental data points were chosen in order to build the error functional Ω. Subcase "a" corresponds to density=1; subcase "b" corresponds to density=0.5; subcase "c" corresponds to density=0.2; subcase "d" corresponds to density=0.1.

The results of sensitivity analysis obtained for the stiffness coefficient *k* and the damping coefficient *c* are summarized in Table 1. Remarkably, the result

of fitting process does not significantly depend on the size and the position of time data interval as well as it is independent of sampling. The coefficient of variation defined as the ratio between the standard deviation and the average value always was lower than 3%. The same sensitivity study was carried out for the experimental data obtained from the second procedure. Analogous qualitative and quantitative results were obtained, but they have not been included here for the sake of brevity.

The results found showing the insensitivity of the procedure to size and position of the interval under study, give confidence on the robustness of the procedure itself. Moreover, the results suggested a criterion for choosing the data interval where to carry out the fitting process. The data interval was set to be the largest in size and with the maximum density by including all possible data points. In general, the largest size of the data time interval is determined by two transient effects at the beginning and end of the vibration period. Experimental data may initially appear irregular just after the instant at which impact occurs because of the transient effect of the impact itself (this is consistent with other study reported in literature: see for example, Fig. 2 of Fukashiro et al [12]). Data relative to the final part of the vibration process when the oscillation is almost completely damped also should be avoided as the signal to noise ratio may get close to 1. By cutting properly the initial and final parts of the data time interval it is possible not to introduce numerical disturbances in the fitting process.

Once the values of the five unknown parameters were determined by minimizing the error functional (29), the values of the stiffness K and damping C of the equivalent vibrating system were calculated with Eqs. (13) and (14) for the first load case. The reaction force f developed in the TS was calculated with Eq.

(16). Equations (17) finally provided the apparent values of stiffness k and damping c of the TS.

For the second loading case, Eq. (16) was again used to evaluate the reaction force f developed in the TS. Finally, Eqs. (25) allowed visco-elastic parameters k and c to be determined.

3.- Results and discussion

The apparent values of stiffness k and damping c were determined for a population including seven males and three females. Each subject was submitted to both loading conditions in order to have a homogeneous basis of comparison between the two measurement protocols. The right leg of each subject was tested as this was the case for which both equipments developed were fully usable. The characteristics of the population in terms of sex, age, height, weight and R/r ratio are summarized in Table 2. For comparison purposes, representative values of populations of Ref [12] and [13] have also been included in Table 2.

As can be seen, the average age of the populations of the three studies is quite similar as well as the size of the population (6 in Ref. [12], 10 in Ref. [13], 10 in the present study). However, whereas height and weight are quite similar in what respect to the present study and reference [13], they both are significantly higher than those corresponding to the population of reference [12].

For each load level, experimental tests were replicated four times to check the level of repeatability of measurements. For that purpose, tests were performed sequentially without altering the general configuration of the testing apparatus and taking a proper time interval lasting several seconds between each replication. In particular, the foot position was unaltered (no repositioning) during these four tests. In this way, although there is a device to reproduce the position of the foot

in the load cell in all tests, uncertainties in the values of R/r are completely avoided.

Figures 12 and 13 show the results obtained in the case of a 30 kg applied weight respectively for the first loading case described by the vertical translation of the lower leg and the second loading case described by the rotation of the foot around the ankle articulation. The plots present the evolution of the reaction force (F) sensed by the load cell during the tests. Experimental data appear superimposed on the corresponding theoretical values predicted by the 1-degree of freedom models to which were given in input the parameter values obtained from the fitting procedure described in Section 2.3. Notice that while in Fig. 12 the value of the signal (F) oscillates around a value in between 41 and 42 kg, in Fig. 13 it oscillates around a value in between 32 and 33 kg. In both figures the applied weight is the same (30 kg), but in the first procedure (Fig. 12) there is an additional oscillating mass of the lower part of the leg that produces an additional weight of around 11 kg, whereas in the second procedure (Fig. 13) the additional weight involved in the oscillation is only around 2.5 kg The figures are relative to Subject 1. Since data trends obtained for the other subjects are very similar they will not be reported in the paper for the sake of brevity.

Results below each plot in Figures 12 and 13 include the steady-state value of the reaction force f_{ss} developed in the triceps surae after the stabilization of the vibration signal. This quantity was obtained from the steady-state force value F_{ss} measured by the load cell (see Fig. 10) and using Eq. (3). The values of apparent stiffness k and viscosity c obtained via least-square fitting are also indicated in the figure. The maximum and minimum values, range of variation, average value, standard deviation and the coefficient of variation for f_{ss}, k and c are reported for both testing protocols. The time interval utilized in the fitting process for each test

replication changed in function of the structure (i.e. shape, quality, etc.) of the signal. Experimental data were pre-processed to remove signal disturbances appearing at the beginning and the end of the measurement period.

By analyzing the force-time plots shown in Figs. 12-13 the presence of a secondary frequency mixed with the fundamental vibration frequency can be observed. The secondary frequency depends on the natural oscillation of the equipment structure and should be at least 2.5 times higher than the MTC frequency in order not to perturb the measured TS frequency (see, for example, Ref. [21]). The natural frequency of the testing apparatus was measured by performing vibration tests without human subjects. The apparatus was submitted to an impulse and the corresponding vibration response was recorded by the load cell. Modifications aimed at increasing the stiffness of the testing apparatus allowed the natural frequency of the structure to be 90-100 rad/s, hence more than three times higher than the MTC natural frequency (20-30 rad/s) registered for the tested subjects. Therefore, the secondary vibration frequency of the structure does not affect significantly the measurement of MTC mechanical properties.

An excellent agreement between the experimental data recorded by the load cell and the numerical results derived from the fitting process can be observed from Figs. 12-13. Therefore, the mechanical behaviour of the vibrating systems entailed by the two experimental setups was efficiently described by the 1-degree of freedom systems developed in Section 2.

The steady-state force f_{ss} developed in the MTC presents a statistical dispersion of about 2% in the case of the first loading case. Negligible dispersion occurs for the four test replications performed in the second load case. The statistical dispersion on f_{ss} can be explained by the fact that modifying the subject's position towards front or back implies variations in the reaction force

that the foot generates on the load cell. The testing apparatus was properly adjusted to minimize this effect which instead is not important for the second loading case as the subject's back lies on the floor.

In the case of the first testing apparatus, the 1.9% coefficient of variation found for the reaction force f_{ss} developed in the triceps surae entails a coefficient of variation equal to 3.4% and 11% for apparent stiffness k and viscosity c, respectively. The higher dispersion found for mechanical properties can be explained in view of the variations in vibration frequency observed for the different replications. Furthermore, the MTC force f_{ss} is proportional to the stiffness which in turns depends on the square of vibration frequency.

For the second loading case, the coefficient of variation for the f_{ss} force dropped to 0% while the values of the coefficient of variation found for the apparent stiffness and viscosity parameters are 5.6% and 19.9%, respectively.

The results obtained for the whole weight range (i.e. between 10 and 40 kg) considered in the experimental campaign carried out in this study is summarized in Tables 3 and 4, as an illustrative example, for Subject 1. The tables list the reaction force f_{ss}, apparent stiffness k and viscosity c and the corresponding average values, standard deviations and coefficients of variation.

In order to better assess the relationships between mechanical properties k and c and the applied weight, average results obtained in the experimental tests are plotted in Figs. 14 and 15, respectively, for apparent stiffness and viscosity (the figures include range bars for the minimum and maximum values). The apparent stiffness k increased with the applied load for all subjects. The same behaviour was seen for both loading cases and can be explained in view of the contribution given to the reaction force by the soleus muscle whose stiffness depends on the magnitude of applied load. The relationship between the viscosity

c and the applied load is less clear than in the case of stiffness. In any case, to assume, as in many simplified models, that viscosity presents a constant value versus the applied load, seems a plausible assumption, in view of the results obtained.

It is clearly shown in figures 14 and 15 that the TS mechanical properties are systematically different when measured using one or the other procedure. To make it even clearer, figure 16 shows the value of the apparent stiffness (for 25 kg) for all subjects measured using both procedures. In particular, figure 16 a) shows absolute stiffness values and figure 16 b) shows the ratio of stiffness values measured by the two procedures (rotation of the foot / vertical displacement). From figure 16 a) it is clear that stiffness values strongly depend on the subject. From figure 16 b) it can be appreciated that the procedure based on the rotation of the foot, systematically yields lower values (approximately 50% in the present study) and this fact shows a strong consistency, as it is almost the same for the ten tested subjects. With reference to viscosity values, the trend observed is similar, the procedure based on the vertical displacements giving systematically higher values than the procedure based on the rotation of the foot.

Table 5 shows the results for the TS stiffness (*k*) obtained for all tested subjects, right leg, and 25 kg of applied weight, using the procedure described in Section 2.1 and Section 2.2. Table 6 show the corresponding results for TS viscosity (*c*), also for the ten tested subjects, right leg and 25 kg. Results for stiffness in Table 5 (1st procedure) indicates that for each subject, a reasonably low dispersion was found in the results. Nevertheless the mean values differ significantly from one subject to another (values varying from 121 kN/m in subject 5 to 272 kN/m in subject 6). The same trend is observed in Table 5 for the procedure based on the rotation of the foot around the ankle articulation. For the

viscosity values (Table 6) it can be observed that higher dispersion was found within each subject (with coefficients of variation up to 28% in the worst case) and also high differences were found between average values for different subjects. It is also remarkable the difference found between both procedures.

Whilst material property values determined from the two measurement protocols analysed in this study were qualitatively similar, they were not comparable at all from a quantitative point of view. However, this does not mean that the two identification procedures should not be used as independent tools to estimate visco-elastic parameters of the triceps surae MTC for a particular person.

Although in contrast with literature data (for example, visco-elastic properties of the human TS quoted in Refs. [12,13] agree also in quantitative terms), the present results sound logical. The differences seen between the two measurement procedures must derive from two reasons. In the first place, the oscillating mass involved in the two load cases (for a nominal value of M_w) is not the same: this affects the response of the MTC and hence the apparent stiffness of the vibrating system. The stiffness of the muscle depends on the force that it is executing, that is, the prestress of the muscle before the movement and this obviously depends (besides the individual and his physical state) on the specific position, weight applied, etc. Secondly, the two measurement protocols rely on a different theoretical foundation: the first procedure considered the vertical translation of the lower leg while the second procedure considered the rotation of the foot around the ankle articulation. This led to have different elements participating in the system response thus altering the vibration frequency which is the basic quantity on which values of mechanical properties depend. In this context, it is noticeable to think of about differences of the common assumption, $M_s \approx M$, made in both procedures. Thus, whereas in the first procedure the

acceleration of all points involved in the movement is basically the same, in the second procedure the acceleration of each point is a function of the distance to the rotation point. All this assigns to the hypothesis made a different level of representativity in each procedure.

4.- Conclusions.

This paper compared two procedures for evaluating in vivo apparent mechanical properties (stiffness and viscosity) of the triceps surae muscle-tendon complex. Experimental measurements, based on the free vibration technique, were conducted using two experimental setups specifically designed. The values of TS visco-elastic parameters were then determined by means of a least-square fitting approach.

Additionally to the design and performance of two devices for measuring TS properties, three main contributions can be highlighted. First, a protocol has been proposed and validated to prove the repeatability of the results for a subject under similar testing conditions. Second, a precise procedure of measurement of the lever arms of the foot has been developed and applied to the subjects studied. Finally, a clarification of the presence of a static mass and a dynamic mass appearing in the experiments (distinction omitted in previous papers) has been carried out.

A good agreement between the experimental data measured by a load cell and the theoretical predictions provided by an equivalent 1-degree of freedom model simulating the dynamic behaviour of the vibrating system was found for both testing protocols. This confirms the feasibility of using the identification procedure developed in this study for many purposes such as, for example, to

compare characteristics of different subjects or, for a single individual, to control the evolution of MTC properties with respect to time, training, etc.

However, the values of visco-elastic parameters found by considering the vertical displacement of the lower leg or the rotation of the foot around the ankle articulation could be compared each other only in qualitative terms. The differences in the measurements obtained using both protocols showed a very convincing consistency. This finding is very important if one considers that in this study the same population was submitted to both load cases. Conversely, literature data that indicated also a quantitative correspondence of visco-elastic properties were obtained by considering completely different populations.

Acknowledgments: The authors acknowledge the financial support of the Junta de Andalucía and Fondo Social Europeo through the Project P08-TEP-04071.

References

[1] Shorten, M. R. (1987). Muscle elasticity and human performance. In: Gheluwe, B. van, and Atha, J. (eds.). *Current research in sports biomechanics*, 1-18.
[2] Horita, T., Komi, P.V., Hämäläinen, I. and Avela, J. (2003). Exhausting stretch-shortening cycle (SSC) exercise causes greater impairment in SSC performance than in pure concentric performance. *Eur J Appl Physiol*, 88, 527-534.
[3] Komi, P.V. (1986) Training of muscle strength and power: interaction of neuromotoric, hipertophic and mechanical factors. *Int J Sports Med Suppl*, 7, 10-5.
[4] Józsa, L.G. and Kannus, P. (1997). Human tendons: Anatomy, physiology and pathology. In: Washbburn, R. and Frey, R. (eds.). Human Kinetics.
[5] Huxley, A. F. and Simmons, R.M. (1971). Proposed mechanism of force generation in striated muscle. *Nature*, 233, 533-538.
[6] Morgan, D. L. (1977). Separation of active and passive components of short-range stiffness of muscle. *Am J Physiol*, 232(1), C45-9.
[7] Rack, P. M. and Westbury, D. R. (1984). Elastic properties of the cat soleus tendon and their functional importance. *J Physiol*, 347, 479-495.
[8] Pousson, M., Hoecke, J. V. and Goubel, F. (1990). Changes in elastic characteristics of human muscle induced by eccentric exercise. *J Biomech*, 23(4), 343-348.
[9] Fukashiro, S., Komi, P. V., Jarvinen, M. and Miyashita, M. (1995a). In vivo achilles tendon loading during jumping in humans. *Eur J Appl Physiol*, 71(5), 453-458.
[10] Fukashiro, S., Itoh, M., Ichinose, Y., Kawakami, Y. and Fukunaga, T. (1995b). Ultrasonography gives directly but noninvasively elastic characteristic of human tendon in vivo. *Eur J Appl Physiol*, 71(6), 555-557.

[11] Lafortune, M. A., Hennig, E. M. and Lake, M. J. (1996). Dominant role of interface over knee angle for cushioning impact loading and regulating initial leg stiffness. *J Biomech*, 29(12), 1523-1529.
[12] Fukashiro, S., Noda, M. and Shibayama, A. (2001). In vivo determination of muscle viscoelasticity in the human leg. *Acta Physiol Scand*, 172(4), 241-248.
[13] Babic, J. and Lenarcic, J. (2004). In vivo determination of triceps surae muscle-tendon complex viscoelastic properties. *Eur J Appl Physiol*, 92(4-5), 477-484.
[14] Faria, A., Gabriel, R., Abrantes, J., Brás, R. and Moreira, H. (2010) Triceps-surae musculotendinous stiffness: Relative differences between obese and non-obese postmenopausal women. *Clin Biomech*, 24, 866-871.
[15] Hill, A. V. (1938). The heat of shortening and the dynamic constants of muscle. Proceedings of the Royal Society of London. *Biological Sciences*, Series B. 126(843), 136-195.
[16] Zatsiorski, V. and Seluyanov, V. (1983). The mass and inertial characteristics of the main segments of the human body. In: Matsui, H. and Kobayahi K (eds). Biomechanics VIII-B, pp 1152-1159. Human kinetics.
[17] Zatsiorsky, V.M., Seluyanov, V.N. and Chugunova, L., (1990). In vivo body segment inertial parameters determination using a gammascanner method. In: Berme, N., Cappozzo, A. (Eds.), Biomechanics of Human Movement: Application in rehabilitation, sports, and ergonomics. Bertec Corporation, Worthington, OH, pp. 187–202.
[18] Donahue, T.L.H., Hull, M.L., Rashid, M.M. and Jacobs, R.C., (2000). A Finite element model of the human knee joint for the study of tibio-femoral contact. *J. Biomech. Eng*. 124, 273-280.
[19] Strickland, M.A., and Taylor, M. (2009). In-silico wear prediction for knee replacements - methodology and corroboration, *Journal of Biomechanics*, 42, 1469- 1474.
[20] París-García, F. (2010). In-vivo determination of the viscoelastic properties of the Triceps Surae by means of the free vibration technique. Ph.D. Thesis (in Spanish). University of Seville.
[21] Clough, R.W. and Penzien, J. (1975). Dynamics of Structures, Prentice-Hall.

Figures

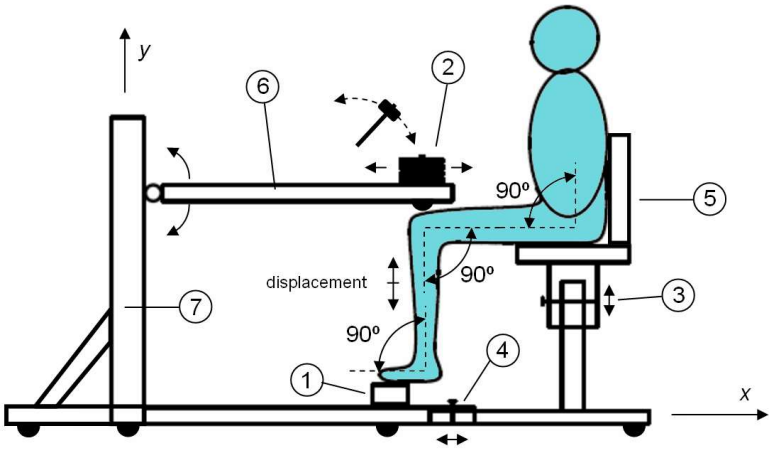

Fig. 1. Schematic of the experimental setup for determining TS visco-elastic properties based on the vertical displacement of the lower leg.

Fig. 2. Global view of the experimental apparatus based on the measurement of lower leg vertical displacements.

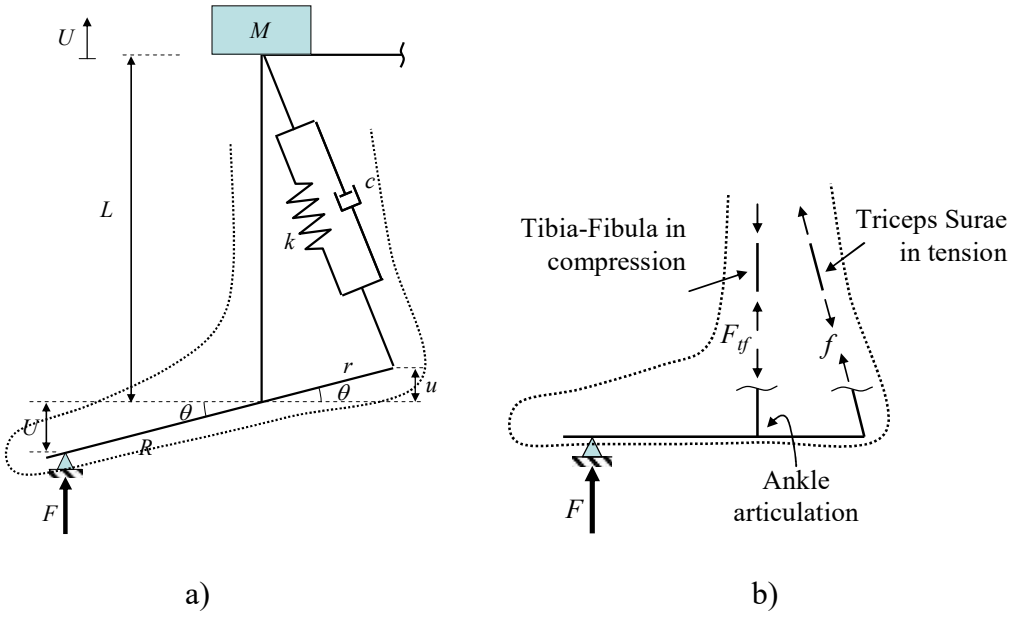

Fig. 3. Experimental setup based on the measurement of the vertical displacement of the lower leg: a) Simplified scheme of an arbitrary position taken in the vibration process; b) Forces involved in the equilibrium around the ankle.

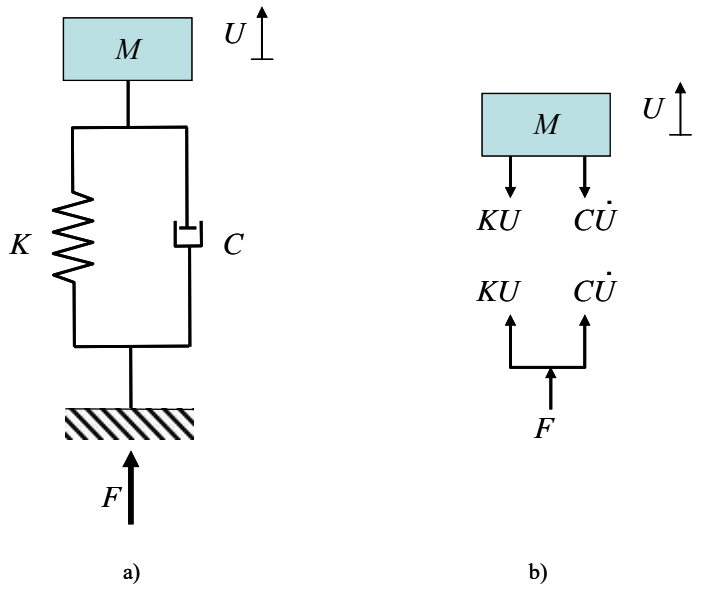

Fig. 4. a) Equivalent dynamic system including one degree of freedom; b) Force diagram.

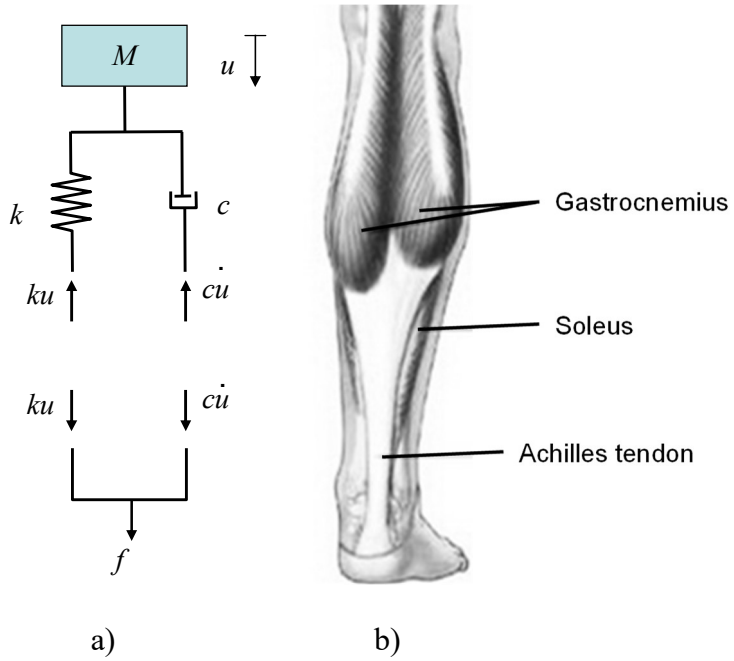

Fig. 5 Force diagram for the equivalent dynamic system of TS muscle-tendon complex.

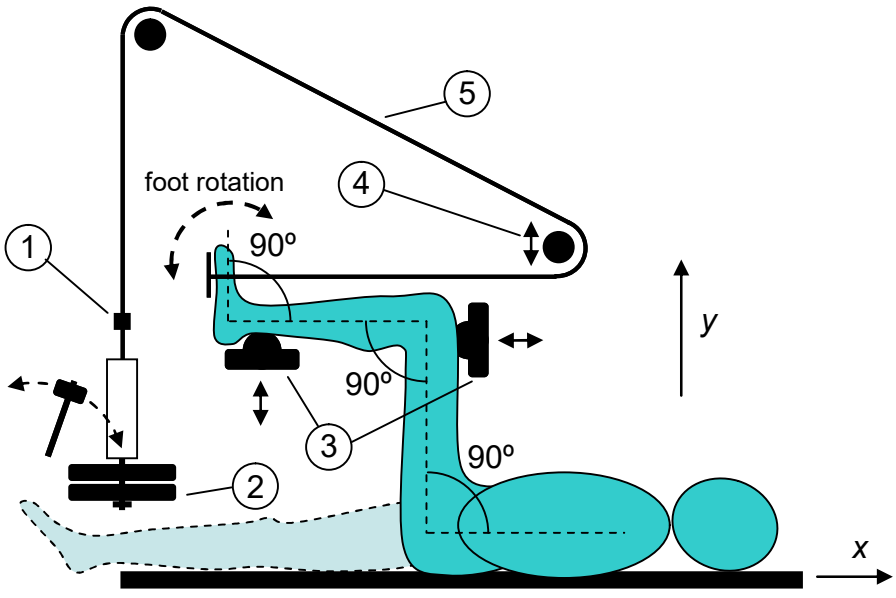

Fig. 6. Schematic of the experimental setup for determining TS visco-elastic properties based on the rotation of the foot around the ankle articulation.

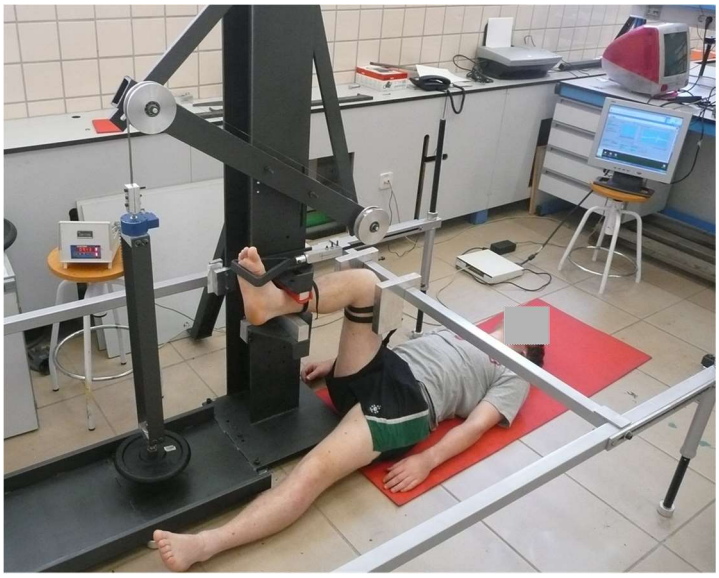

Fig. 7. Global view of the experimental apparatus based on the measurement of the rotation of the foot around the ankle articulation.

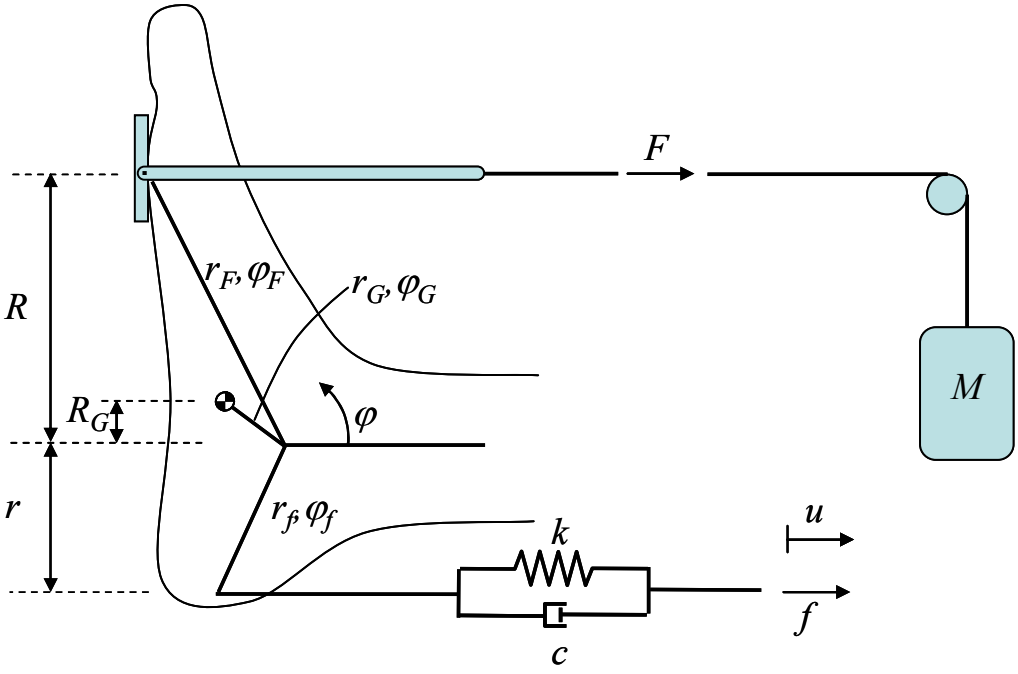

Fig. 8. Experimental setup based on the measurement of the rotation of the foot around the ankle articulation: simplified scheme of the foot functioning during the free vibration.

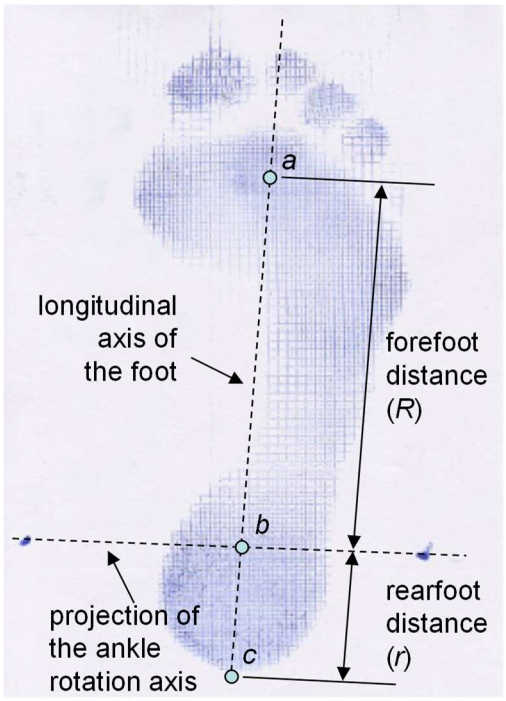

Fig. 9. Forefoot and rearfoot distances measurements by means of a pedigraphy.

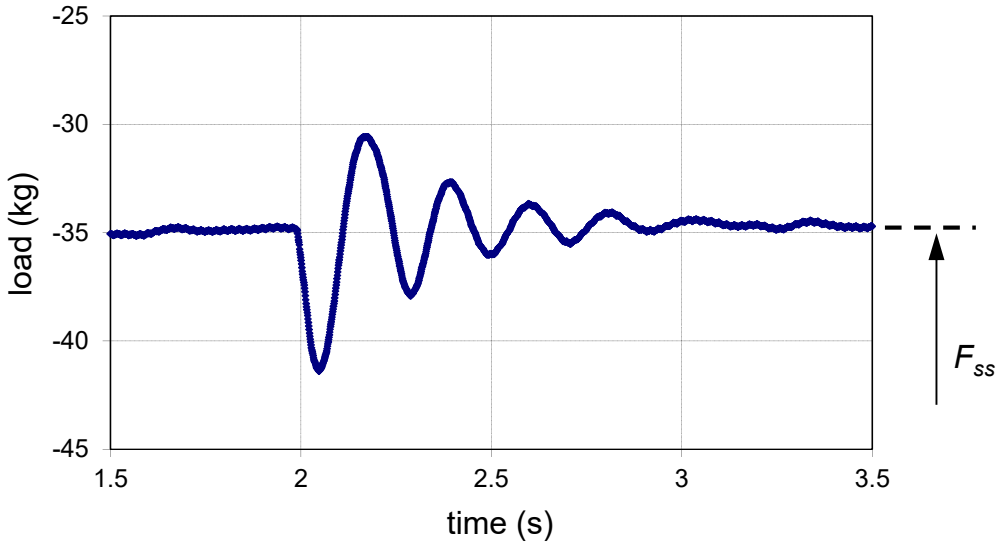

Fig. 10. Typical force-time diagram registered by the load cell.

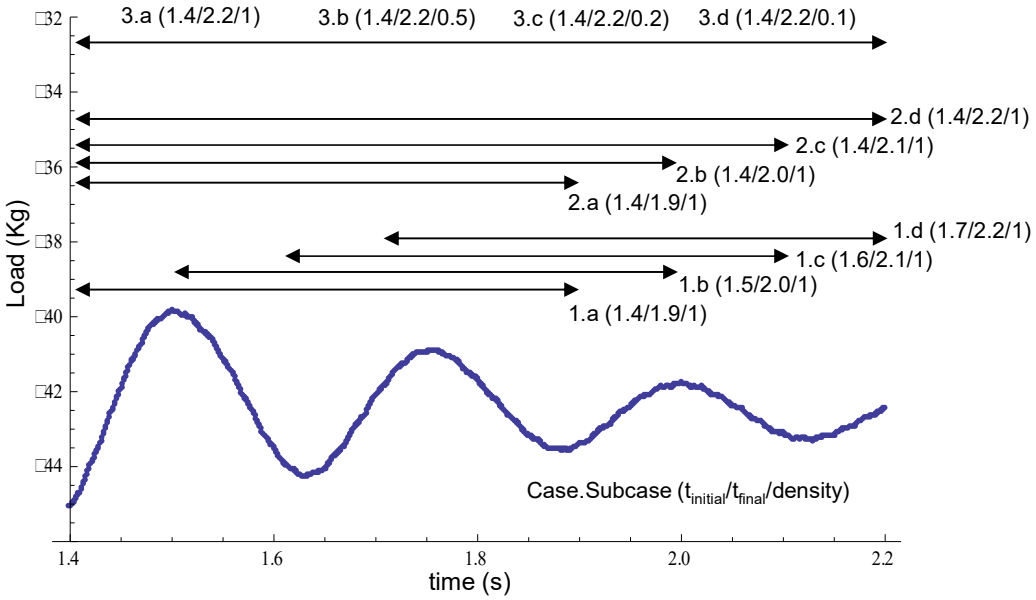

Fig. 11. Sensitivity parameters analyzed in order to optimize the fitting process.

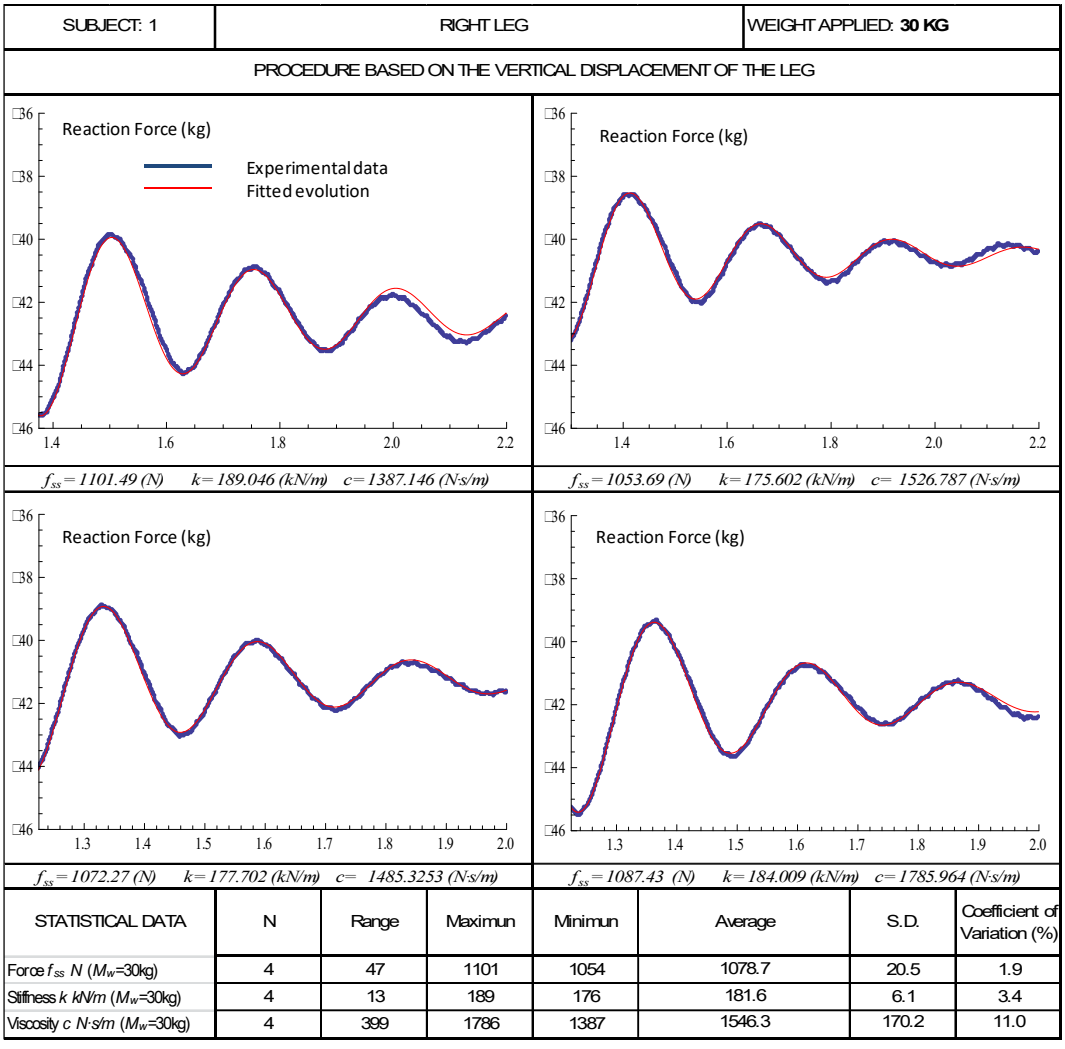

STATISTICAL DATA	N	Range	Maximun	Minimun	Average	S.D.	Coefficient of Variation (%)
Force f_{ss} N (M_w=30kg)	4	47	1101	1054	1078.7	20.5	1.9
Stiffness k kN/m (M_w=30kg)	4	13	189	176	181.6	6.1	3.4
Viscosity c N·s/m (M_w=30kg)	4	399	1786	1387	1546.3	170.2	11.0

Fig. 12. Reaction force F *vs* time results obtained for Subject 1 for the loading case based on the measurement of the vertical displacement of the right leg.

SUBJECT: 1	RIGHT LEG	WEIGHT APPLIED: **30 KG**

PROCEDURE BASED ON THE ROTATION OF THE FOOT AROUND THE ANKLE

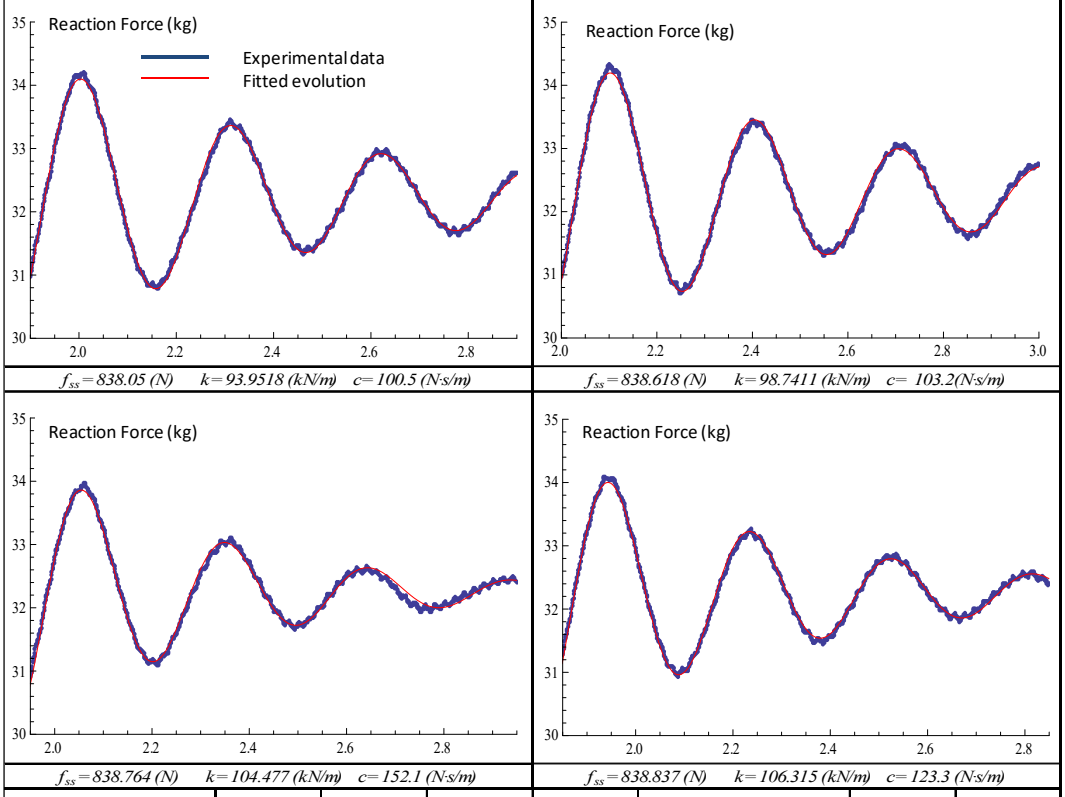

f_{ss} = 838.05 (N) k = 93.9518 (kN/m) c = 100.5 (N·s/m)

f_{ss} = 838.618 (N) k = 98.7411 (kN/m) c = 103.2(N·s/m)

f_{ss} = 838.764 (N) k = 104.477 (kN/m) c = 152.1 (N·s/m)

f_{ss} = 838.837 (N) k = 106.315 (kN/m) c = 123.3 (N·s/m)

STATISTICAL DATA	N	Range	Maximun	Minimun	Average	S.D.	Coefficient of Variation (%)
Force f_{ss} N (M_w=30kg)	4	1	839	838	838.6	0.4	0.0
Stiffness k kN/m (M_w=30kg)	4	12	106	94	100.9	5.6	5.6
Viscosity c N·s/m (M_w=30kg)	4	51	152	101	119.8	23.8	19.9

Fig. 13. Reaction force F *vs* time results obtained for Subject 1 in the loading case based on the measurement of the rotation of the foot around the ankle.

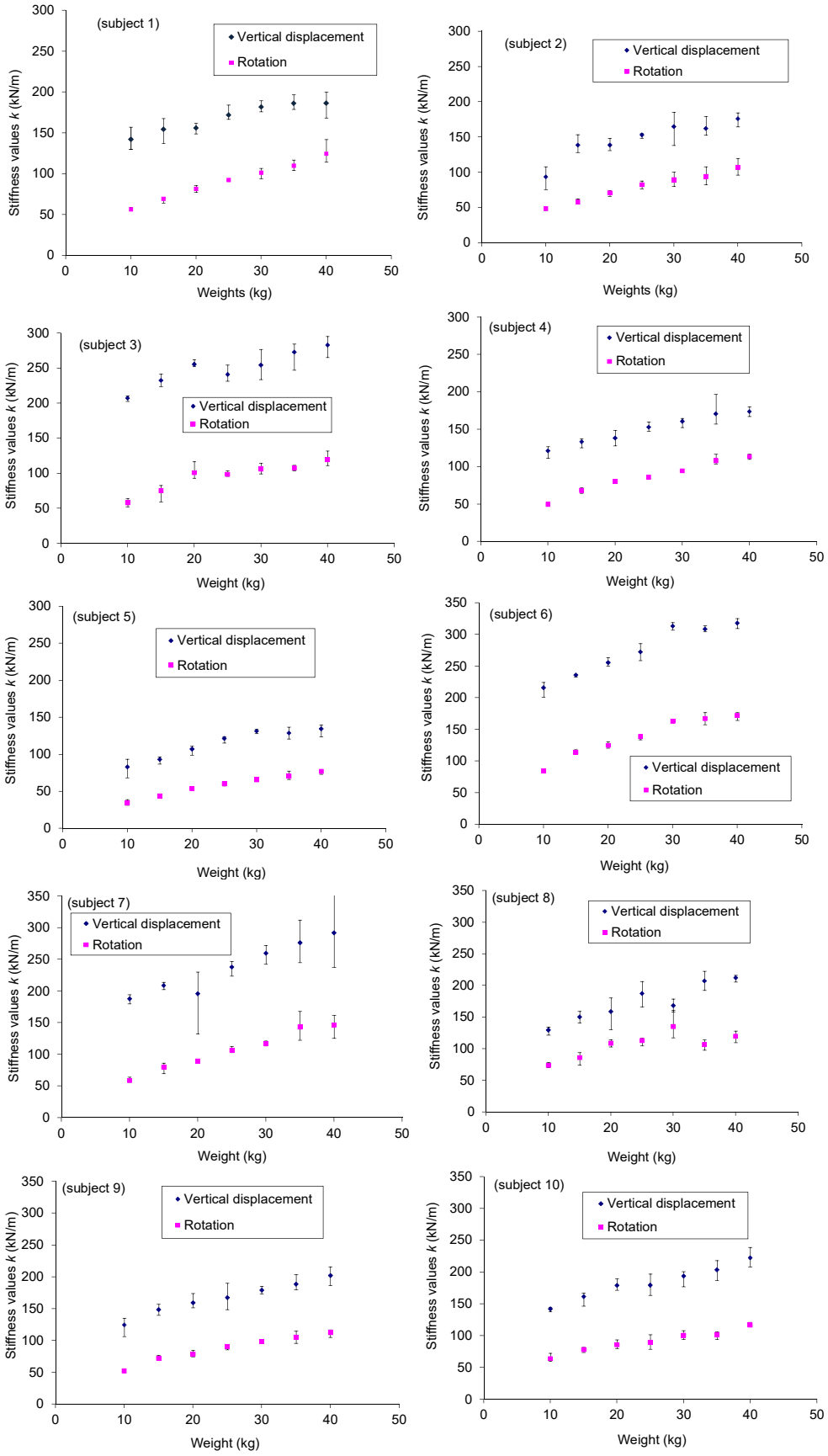

Fig. 14. Variation of the apparent stiffness of TS complex with respect to the nominal applied load for the two measurement protocols and for the ten tested subjects..

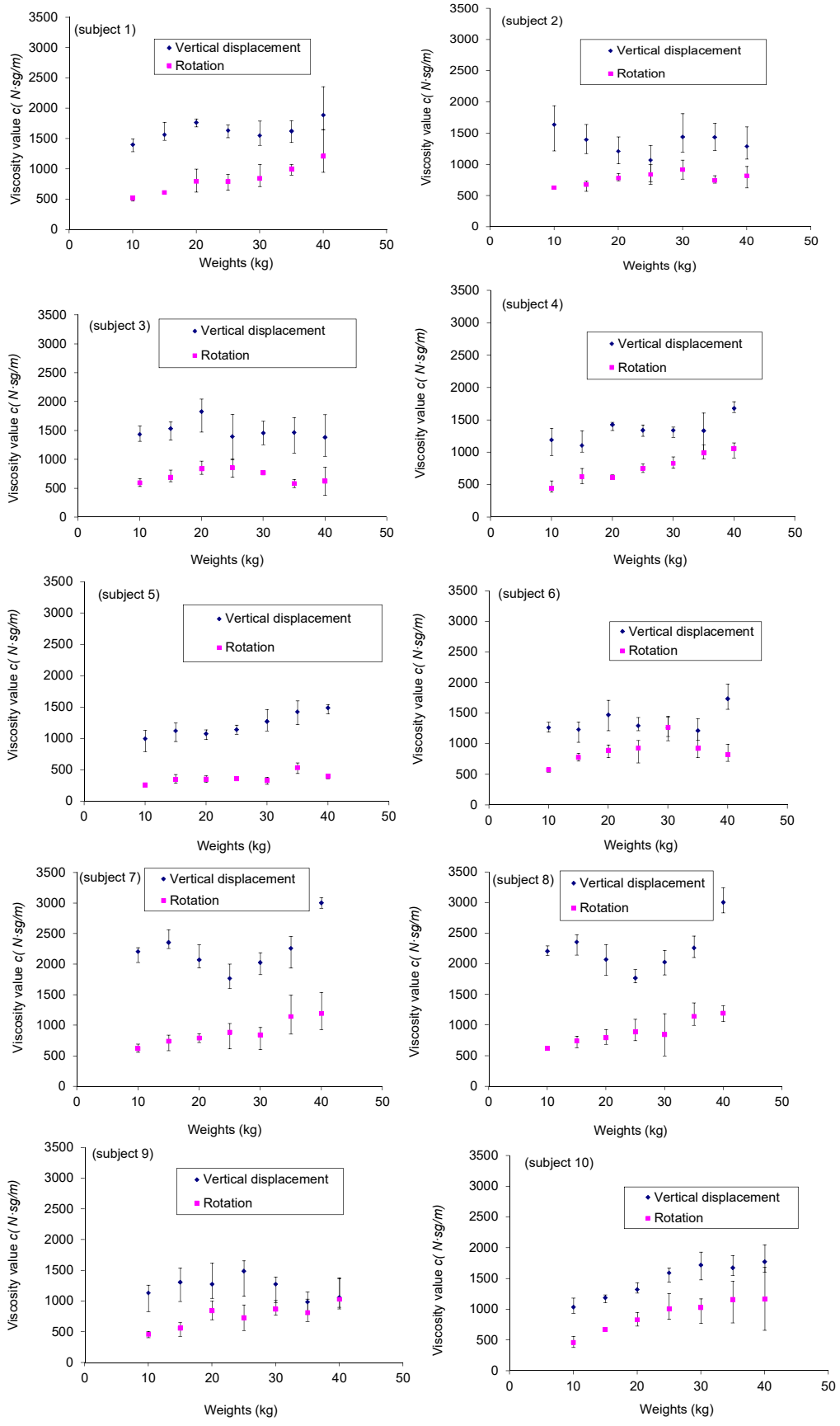

Fig. 15. Variation of the apparent viscosity of TS complex with respect to the nominal applied load for the two measurement protocols and for the ten tested subjects.

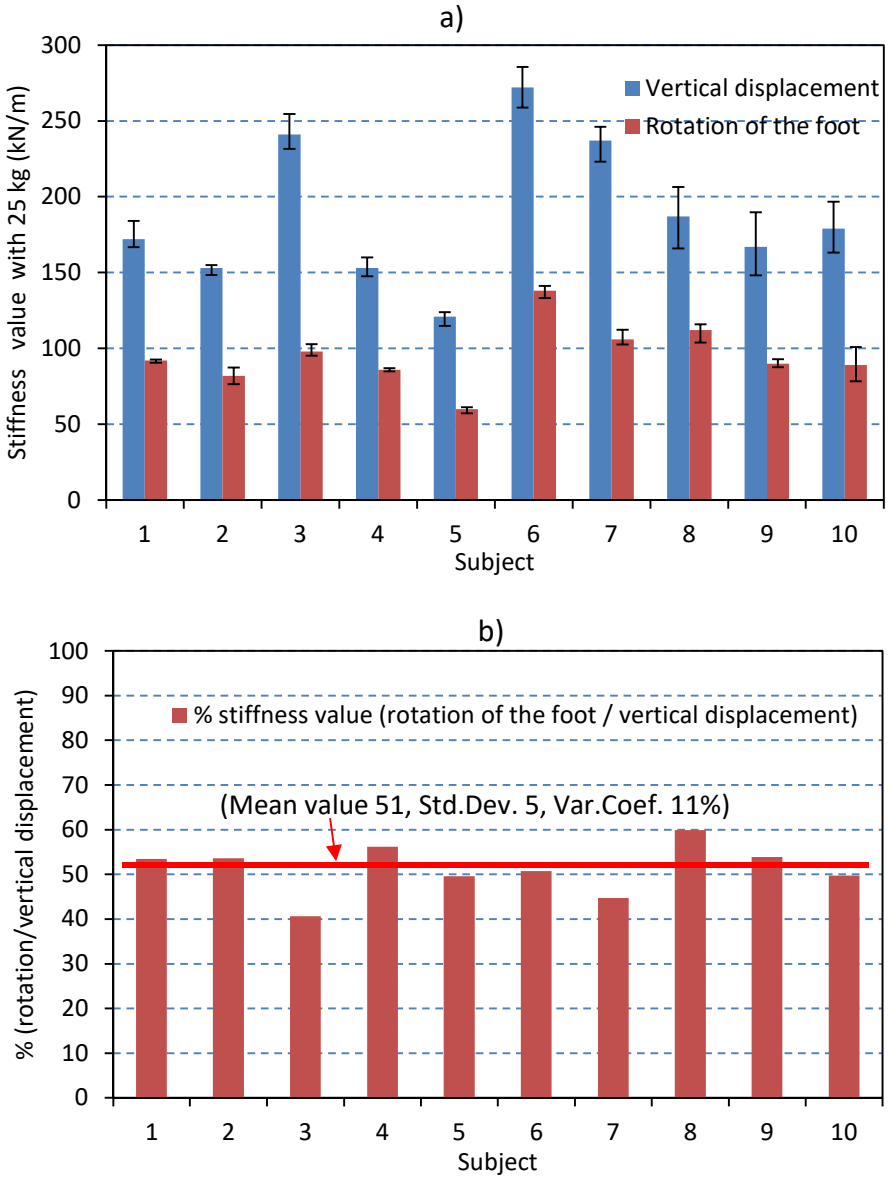

Fig. 16. Variation of the apparent viscosity of TS (25 kg of applied load) for the two measurement protocols and for the ten tested subjects, a) absolute apparent values, b) relative values.

Table 1. Values of *k* and *c* obtained in the parametric study.

	Values of *k* (kN/m)						
	a	b	c	d	Mean	Std.Dev.	CV[(1)] (%)
Case 1	187.34	189.84	195.62	195.59	192.10	4.17	2.17
Case 2	187.34	187.73	189.04	188.75	187.47	1.96	1.05
Case 3	188.75	188.74	188.72	188.68	188.72	0.03	0.02

(1) CV: Coefficient of Variation

	Values of *c* (N·s/m)						
	a	b	c	d	Mean	Std.Dev.	CV[(1)] (%)
Case 1	1216.3	1290.7	1376.3	1657.8	1385.3	193.09	13.94
Case 2	1216.3	1288.2	1387.4	1290.4	1295.5	70.23	5.42
Case 3	1290.4	1289.5	1286.5	1281.9	1287.1	3.79	0.29

(1) CV: Coefficient of Variation

Table 2. Characteristics (sex, age, height, weight and *R*/*r* ratio) of the tested subjects.

Subject	sex	age (years)	height (m)	weight (kg)	*R*/*r*
1	male	34	1,88	95	2,65
2	male	21	1,76	75	2,71
3	male	32	1,94	98	2,93
4	male	21	1,75	77	2,59
5	male	37	1,78	84	2,17
6	male	24	1,75	80	3,12
7	male	29	1,74	70	2,97
8	female	31	1,73	54	2,94
9	female	31	1,6	56	2,64
10	female	32	1,72	60	2,61
Reference	Population	Mean/Std.Dev.	Mean/Std.Dev.	Mean/Std.Dev.	
Present work	7 males 3 females	29 / 5,5	1,77 / 0,09	74,9 / 15,2	
Ref. [12]	4 males 2 females	25 / 1,9	1,63 / 0,06	60,2 / 5,7	
Ref. [13]	10 males	26 / 4,0	1,80 / 0,06	77,1 / 7,2	

Table 3. Results obtained for the force developed in the TS complex by considering the vertical displacement of the lower leg (Subject 1).

values of f_{ss}, k and c		TEST NUMBER						
		TEST 1	TEST 2	TEST 3	TEST 4	**Average**	**S.D.**	**C.V.**
10 kg	f_{ss}	560	563	582	610	579	22.7	3.9
	k	139	130	143	157	142	11	8
	c	1291	1430	1245	1444	1353	99.8	7.4
15 kg	f_{ss}	683	695	735	737	712	28	4
	k	137	153	159	167	154	13	8
	c	1468	1713	1442	1426	1512	135.1	8.9
20 kg	f_{ss}	797	813	827	844	820	20	2
	k	148	156	157	162	156	5	4
	c	1669	1639	1767	1750	1706	61.9	3.6
25 kg	f_{ss}	946	975	983	983	972	18	2
	k	166	170	184	166	172	8	5
	c	1668	1578	1466	1604	1579	84.6	5.4
30 kg	f_{ss}	1054	1072	1087	1101	1079	21	2
	k	189	176	178	184	182	6	3
	c	1387	1527	1485	1786	1546	170.2	11.0
35 kg	f_{ss}	1114	1124	1152	1169	1140	25	2
	k	178	184	185	196	186	8	4
	c	1735	1596	1391	1556	1570	141.8	9.0
40 kg	f_{ss}	1199	1230	1258	1305	1248	45	4
	k	168	188	200	189	186	13	7
	c	1673	1747	2284	1597	1825	311.7	17.1

Table 4. Results obtained for the force developed in the TS complex by considering the rotation of the foot around the ankle articulation (Subject 1).

values of f_{ss}, k and c		TEST NUMBER						
		TEST 1	TEST 2	TEST 3	TEST 4	**Average**	**S.D.**	**C.V.**
10 kg	f_{ss}	363	363	363	364	363	0.4	0.1
	k	55	59	55	55	56	1.7	3.0
	c	534	511	488	453	496	34.8	7.0
15 kg	f_{ss}	488	488	489	490	489	0.8	0.2
	k	69	64	71	71	69	3.4	5.0
	c	582	599	599	574	588	12.6	2.1
20 kg	f_{ss}	599	600	600	601	600	1.0	0.2
	k	77	82	85	80	81	3.6	4.4
	c	725	965	597	774	765	152.3	19.9
25 kg	f_{ss}	726	726	726	728	727	0.9	0.1
	k	92	92	91	93	92	0.9	1.0
	c	625	879	744	809	764	108.1	14.2
30 kg	f_{ss}	838	839	839	839	839	0.4	0.0
	k	94	99	104	106	101	5.6	5.6
	c	706	725	1069	866	841	167.4	19.9
35 kg	f_{ss}	963	964	964	966	964	1.3	0.1
	k	104	108	117	110	110	5.4	4.9
	c	970	1035	995	869	967	70.9	7.3
40 kg	f_{ss}	1080	1082	1083	1083	1082	1.2	0.1
	k	114	127	115	142	124	13.0	10.4
	c	1153	913	1024	1590	1170	296.7	25.4

Table 5. Results obtained for the TS equivalent stiffness (k) for the tested subjects (with 25 kg).

25 kg	Triceps Surae stiffness using 1st procedure (vertical displacement)						
	Stiffness k (kN/m) for each test				Statistics		
Subject	T1	T2	T3	T4	Mean Value	Std.Dev.	CV (%)
S1	166	170	184	166	171,5	8,5	5,0
S2	148	154	155	154	152,8	3,2	2,1
S3	231	232	245	254	240,5	11,0	4,6
S4	149	160	147	154	152,5	5,8	3,8
S5	122	124	124	115	121,3	4,3	3,5
S6	259	273	285	271	272,0	10,6	3,9
S7	239	223	240	246	237,0	9,8	4,1
S8	200	175	166	206	186,8	19,3	10,3
S9	156	190	174	148	167,0	18,8	11,3
S10	166	163	197	190	179,0	17,0	9,5
TOTAL					**188,0**	**47,1**	**25,1**

25 kg	Triceps Surae stiffness using 2nd procedure (rotation of the foot)						
	Stiffness k (kN/m) for each test				Statistics		
Subject	T1	T2	T3	T4	Mean Value	Std.Dev.	CV (%)
S1	92	92	91	93	92,0	0,8	0,9
S2	83	76	81	87	81,8	4,6	5,6
S3	96	95	98	103	98,0	3,6	3,6
S4	87	85	87	84	85,8	1,5	1,7
S5	57	61	61	60	59,8	1,9	3,2
S6	141	138	140	133	138,0	3,6	2,6
S7	103	106	103	112	106,0	4,2	4,0
S8	116	116	113	104	112,3	5,7	5,1
S9	91	93	88	87	89,8	2,8	3,1
S10	101	88	79	89	89,3	9,0	10,1
TOTAL					**95,3**	**20,7**	**21,7**

Table 6. Results obtained for the TS equivalent viscosity (c) for the tested subjects (with 25 kg).

25 kg	Triceps Surae viscosity using 1st procedure (vertical displacement)						
	Viscosity c (N·s/m) for each test				Statistics		
Subject	T1	T2	T3	T4	Mean Value	Std.Dev.	CV (%)
S1	1720	1627	1511	1653	1627,8	87,1	5,4
S2	1301	976	1306	681	1066,0	299,5	28,1
S3	991	1418	1381	1777	1391,8	321,4	23,1
S4	1423	1293	1389	1244	1337,3	83,0	6,2
S5	1154	1118	1067	1215	1138,5	62,2	5,5
S6	1243	1427	1212	1271	1288,3	95,6	7,4
S7	1482	2002	1722	1848	1763,5	219,8	12,5
S8	813	880	1212	1005	977,5	175,4	17,9
S9	1077	1638	1656	1562	1483,3	273,9	18,5
S10	1635	1670	1441	1602	1587,0	101,2	6,4
TOTAL					**1366,1**	**255,9**	**18,7**

25 kg	Triceps Surae viscosity using 2nd procedure (rotation of the foot)						
	Viscosity c (N·s/m) for each test				Statistics		
Subject	T1	T2	T3	T4	Mean Value	Std.Dev.	CV (%)
S1	644	906	767	834	787,8	111,4	14,1
S2	835	722	801	997	838,8	115,6	13,8
S3	903	1011	806	689	852,3	137,3	16,1
S4	817	719	687	767	747,5	56,8	7,6
S5	338	366	332	390	356,5	26,8	7,5
S6	1051	956	999	686	923,0	162,7	17,6
S7	1026	916	613	983	884,5	186,6	21,1
S8	504	824	662	475	616,3	161,0	26,1
S9	717	934	519	734	726,0	169,6	23,4
S10	1252	1018	836	895	1000,3	184,2	18,4
TOTAL					**773,3**	**182,1**	**23,5**